General Disclaimer

One or more of the Following Statements may affect this Document

- This document has been reproduced from the best copy furnished by the organizational source. It is being released in the interest of making available as much information as possible.

- This document may contain data, which exceeds the sheet parameters. It was furnished in this condition by the organizational source and is the best copy available.

- This document may contain tone-on-tone or color graphs, charts and/or pictures, which have been reproduced in black and white.

- This document is paginated as submitted by the original source.

- Portions of this document are not fully legible due to the historical nature of some of the material. However, it is the best reproduction available from the original submission.

CI8-35506 PR13

CALCULATION OF FLOW ABOUT POSTS AND POWERHEAD MODEL

Interim Report, Contract NAS8-35506

CI-IR-0079

Prepared For:

National Aeronautics and Space Administration
George C. Marshall Space Flight Center
Marshall Space Flight Center, AL 35812

By:

Peter G. Anderson
Richard C. Farmer

CONTINUUM, Inc.
4715 University Drive
Suite 118
Huntsville, AL 35805

January 21, 1985

TABLE OF CONTENTS

TABLE OF FIGURES

FORWARD

This document was prepared by personnel at Continuum, Inc. for NASA-MSFC under Contract NAS8-35506. This document is an interim report on the first year of work under this contract.

1. INTRODUCTION

1.1 Backgroumd

The highly non-uniform flow around the LOX posts in the SSME powerhead has contributed to a long history of failures of the posts. Both pressure and heating loads have caused problems which have resulted in undesirable, but necessary, design modifications such as the use of LOX post flow shields. The geometric complexity of the LOX post flowfield is enormous; 600 posts are fed by the five hot gas discharge ducts from the HPFTP and HPOTP. The posts are fluted to modify the structure of the trailing vortices and are shielded by plates covering pairs of posts in the outermost row. Hot gases flow along the sides of the injector elements into entry ports which conduct the flow through an annulus into the main combustion chamber. The region of posts which are subjected to extreme environments is contained within the region bounded by the exits of the hot gas transfer ducts, the bottom of the oxidizer manifold, and the space above the secondary plate. The hydrogen cavity flow between the primary and secondary plates does not cause severe environments and is not considered further.

Assuming that the flow from the HGM is symmetric about a plane through the center transfer tube, one-half of the region could be modeled at one time. Even the half-plane flow would be too complex to provide a direct numerical solution to the flow field of interest. Continuum has been contracted to address this problem by a phased effort which first models the flow around a single and small clusters (2-10) of posts, second models the velocity field in the cross-flow plane, and third models the entire flow region with a 3-dimensional network-type model. However, the contract has been modified to include a full 3-D numerical solution of the flow field in the high pressure fuel turbopump turnaround duct (TAD), hot gas manifold (HGM) and transfer tubes. The results of this

effort will be used to define boundary conditions for LOX post analyses.

1.2 Objectives

The following sections discuss the work performed under Phase I of the contract as modified to reflect the TAD/HGM/Duct analysis. These sections include a presentation of Continuum's laminar and turbulent boundary layer development in support of the LOX post study and the results of the 3-D HGM analysis.

2. SUMMARY

Continuum has developed shear stress wall functions which will permit viscous analyses without requiring excessive numbers of computational grid points. These wall functions, laminar and turbulent, have been compared to standard Blasius solutions and are directly applicable to the cylinder-in-crossflow class of problems to which the LOX post problem belongs. The results of this work are presented herein.

Continuum has also performed a full 3-D fluid flow analysis of the HPFTP exhaust system which consists of the turnaround duct, 2-duct hot gas manifold and the "Version B" transfer ducts. The results of this analysis are presented in this report.

3. HIGH REYNOLDS NUMBER CROSSFLOW ABOUT A CYLINDER

3.1 Introduction

In order to accurately account for pressure loading and heating to cylinders in crossflow, like for the LOX posts in the powerhead, a detailed flowfield prediction and suitable wall boundary conditions are required. It is impractical to resolve the flowfield in the vicinity of the wall with enough grid points to accurately calculate either the wall friction or heating, therefore a special wall treatment is required. "Wall functions" are commonly used to provide the required boundary conditions; however, care must be exercised in order not to make the wall functions too empirical. The end result is to predict

frictional losses from the detailed flow vectors, not from the mean channel flow. The following procedure was developed and tested with geometrically simple problems to provide the necessary CFD tools for powerhead analysis.

3.2 Laminar Boundary Layers

Laminar boundary layers on a flat plate were analyzed with Continuum's VAST code for constant density and temperature (hence pressure also) conditions. Figure 3-1 shows the results of these analyses compared to the Blasius solution. A mean lateral velocity was used as a boundary condition on the free-stream side of the computational region. The excellent agreement of the VAST solution with the Blasius solution suggests that no significant artificial viscosity effects are present in the solution for this case. Notice that only 15 lateral node points were used for this calculation. Identical results were obtained for a case run with 11 nodes, only one of which was initially in the boundary layer. When 7 nodes were used with a step velocity profile a solution was generated, but the accuracy of this solution was reduced. These results are considered acceptable, and the use of at least one node in the initial boundary layer is reasonable.

3.3 Turbulent Boundary Layer

For turbulent wall flows, including fully developed pipe flows, for a smooth wall the following empirical velocity profiles are valid.

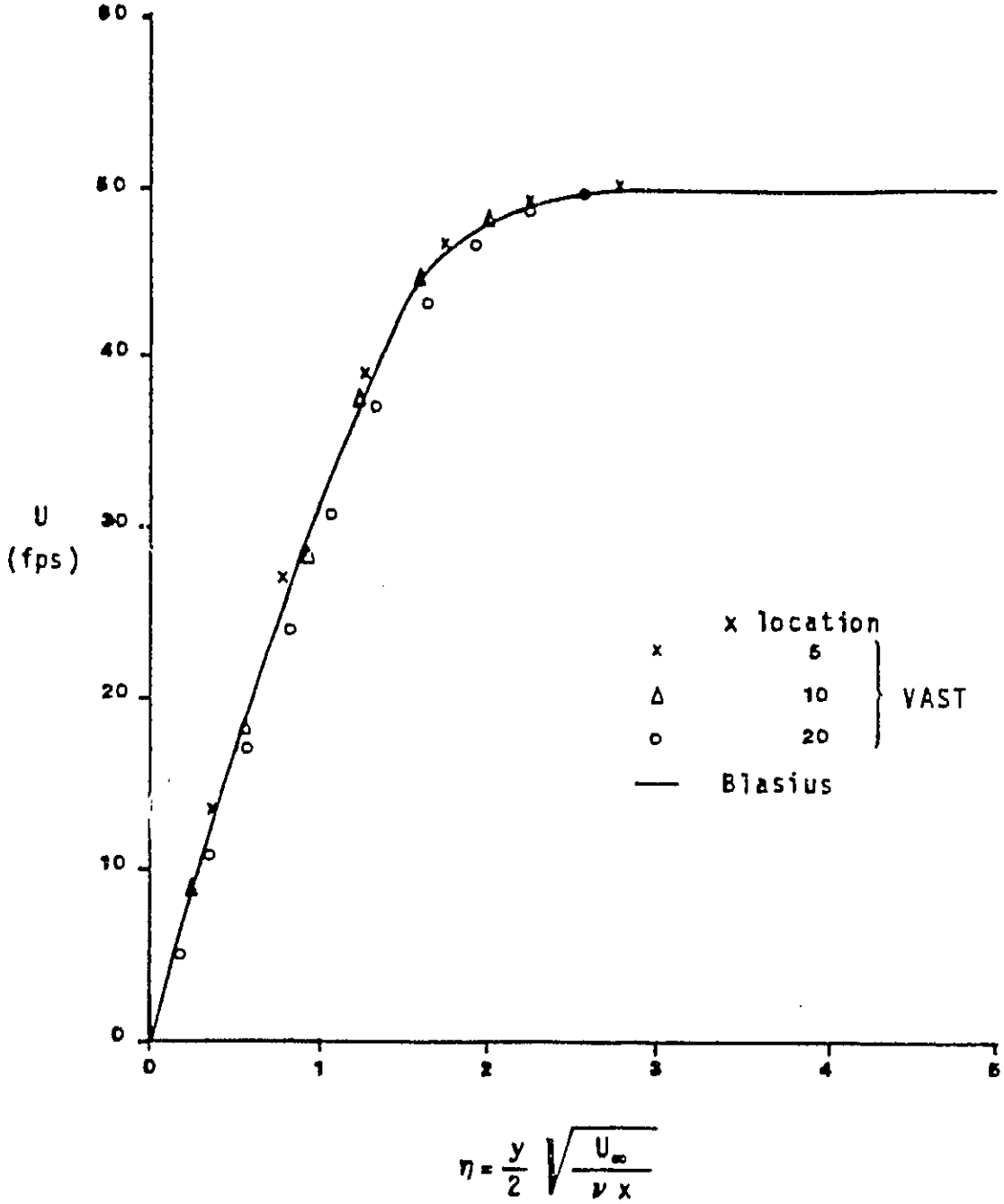

Fig. 3-1 Laminar Boundary Layer on a Flat Plate

$$u^+ = 5.5 + 2.5 \ln(y^+) \quad \text{for } y^+ > 30 \tag{3-1}$$

$$u^+ = -3.05 + 5.0 \ln(y^+) \quad \text{for } 5 < y^+ < 30 \tag{3-2}$$

$$u^+ = y^+ \quad \text{for } y^+ < 5 \tag{3-3}$$

where

$$u^+ = u/u^*$$

$$u^* = (\tau_o/\rho)^{0.5}$$

$$y^+ = (\tau_o/\rho)^{0.5}\, y/\nu$$

Blasius' empirical shear stress relationship is appropriate.

$$\tau_o = 0.0255\, \rho u^2 (\nu/u^* \ell)^{0.25} \tag{3-4}$$

where = R for pipe flow

= δ for boundary layers

The boundary layer thickness implied by (3-4) and a 1/7 power-low profile is

$$\delta = 0.376\, X/R_e^{0.2} \tag{3-5}$$

From equation (3-3)

$$\left(\frac{\partial u}{\partial y}\right)_w = \tau_o/\rho = (u^*)^2/\nu \tag{3-6}$$

In terms of real distance from the wall, equation (3-1) represents most of the boundary layer, therefore the following computation procedure is suggested. A fictitous wall is assumed to be 0.0005 feet away from the real wall, and no flow is assumed to occur between the two walls. Equation (3-1) is valid at .0005 feet from the wall; hence, if u is calculated with a slip boundary condition, u^* is determined. Equation (3-6) is used to

calculate the velocity gradient at the wall. Since equation (3-1) is not explicit in u^*, the approximation

$$u^* = 0.1662529\ u^{0.867325}/(y/\nu)^{0.132675} \qquad (3-7)$$

is used. These equations determine the velocity gradient and shear stress at the wall. An eddy viscosity is used to determine both the local shear stress and the variation of this stress with distance from the wall, y.

$$\mu_T = 0.07\ u^* \ell (FR) + \mu \qquad (3-8)$$

where

$$FR = (y/0.3\ \ell) \text{ for } 0 < (y/\ell) < 0.3$$
$$FR = 1.0 \text{ for } (y/\ell) > 0.3$$

Equations (3-7) and (3-8) and the momentum equations were used to calculate the turbulent boundary layer over a flat plate between 1 and 2 ft running length over the plate. A turbulent boundary layer was assumed at the leading edge of the plate. The flow was air with a free steam velocity of 100 fps (this is an approximate Reynolds Number of 10^6). By adjusting the constants in equations (3-7) and (3-8), the profile at the end of the plate was predicted to be that shown in Fig. 3-2. The fit is very good, especially near the wall; the calculated wall shear stress is within 5% of the correct answer. This procedure is accurate enough to extend its development to more geometrically complex flows. The reasons for the necessity of adjusting the constants in equations (3-7) and (3-8) and for the lack of better fit at y's near the free stream side of the boundary layer are still under investigation.

Research to continue these analyses until cylinders in cross-flow can be accurately simulated is in progress.

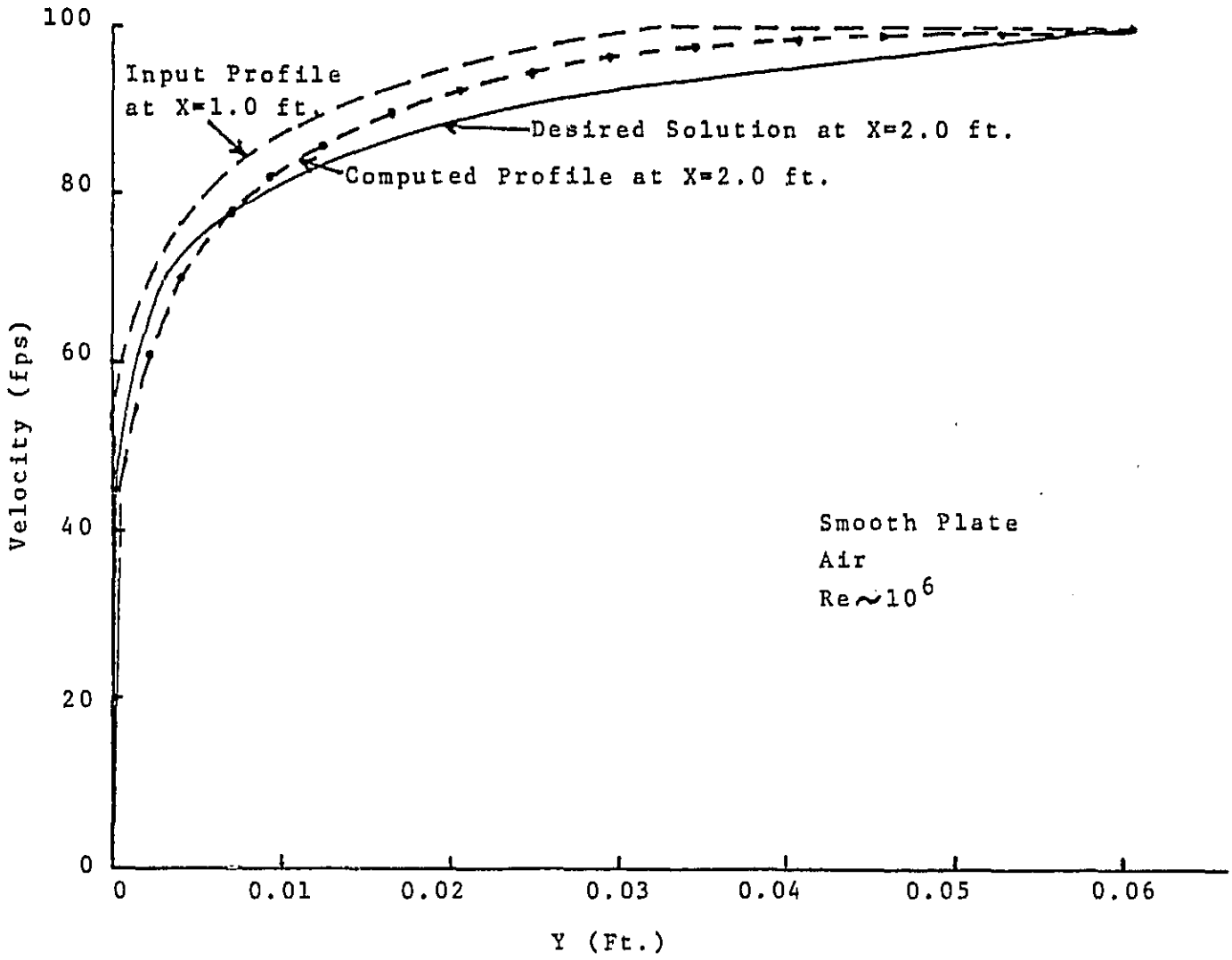

Fig. 3-2 Turbulent Boundary Layer Calculation

4. HGM FLOW ANALYSIS

4.1 Introduction

The analysis of the flow environment surrounding the SSME LOX posts requires a definition of the flow field in the HPFTP transfer tubes exit planes. The exit plane flow is development by defining the flow conditions immediately downstream of the turbine and computing the flow field through the turnaround duct, hot gas manifold and transfer tube. This section discusses the computation of the flow field in the turnaround duct, hot gas manifold and transfer duct for a two-duct configuration.

4.2 Configuration

The configuration analyzed consisted of the FMOF turnaround duct, the "Phase 3" two-duct hot gas manifold and the "Version B" transfer tube which includes the flow separator. The effects of turbine-induced swirl were neglected at the direction of the customer; hence, a plane of symmetry between the 2 transfer tubes was incorporated.

4.3 Flow Conditions at Inlet

The flow conditions at the inlet to the turnaround duct were specified by the customer. The fluid in the system was air at 530°R flowing at 72 lbm/sec. The pressure across the inlet was described by the equation.

$$P = \left[190.0\ \ 0.98 + 0.0441\ \mathrm{Sin}^2\left(\frac{\phi}{2}\right)\right] \text{psia} \qquad (4\text{-}1)$$

where ϕ is the angular location which ranges from 0° between the transfer tubes and 180° on the plane of symmetry on the side fartherest from the transfer tubes. The velocity profile in the TAD inlet is defined by the equation

$$V = \bar{V}(1.0 + 0.04\ \mathrm{Cos}\phi) \qquad (4\text{-}2)$$

where V is the average velocity of any angle ϕ and $\bar{V}$ is the average velocity over the entire inlet. The velocity has no cross flow component due to the assumption of no turbine-induced swirl. The turbulent viscosity was specified as 10,000 times the molecular viscosity for air.

4.4 Computational Grid

The configuration described in subsection 4.2 was modeled using 10,724 nodal grid points. The grid points depicting the boundaries of the configuration are shown in Figs. 4-1, 4-2. The struts and posts in the turnaround duct have been darkened in to clarify their locations. The computational grid in the plane of symmetry at the 0° (between the transfer tubes) and 180° (far side) positions are shown in Fig. 4-3. The inlet to the turnaround duct has been artifically moved upstream to avoid influencing the flow in the 180° bend by the prescribed inlet flow conditions. Figures 4-1 through 4-3 illustrate that all of the salient features of the configuration have been incorporated into the grid.

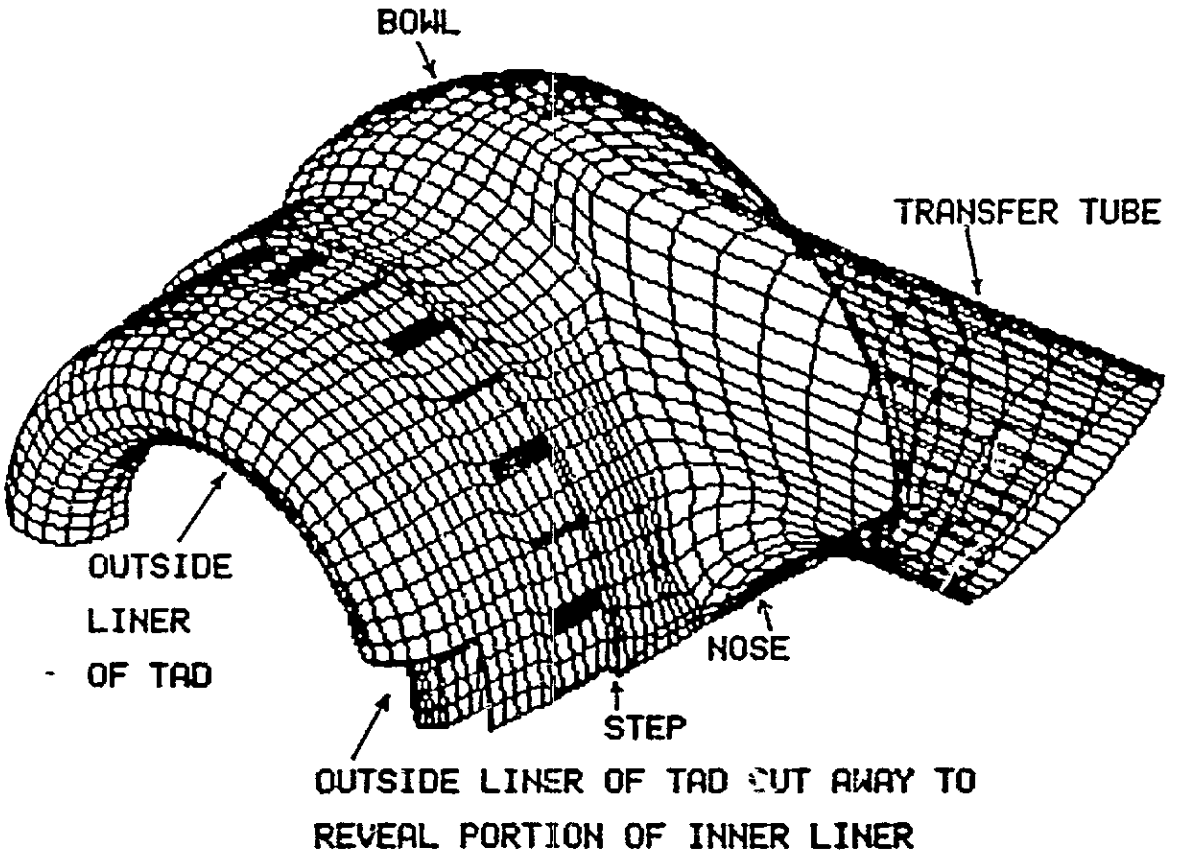

Fig. 4-1 View of Grid From Outside

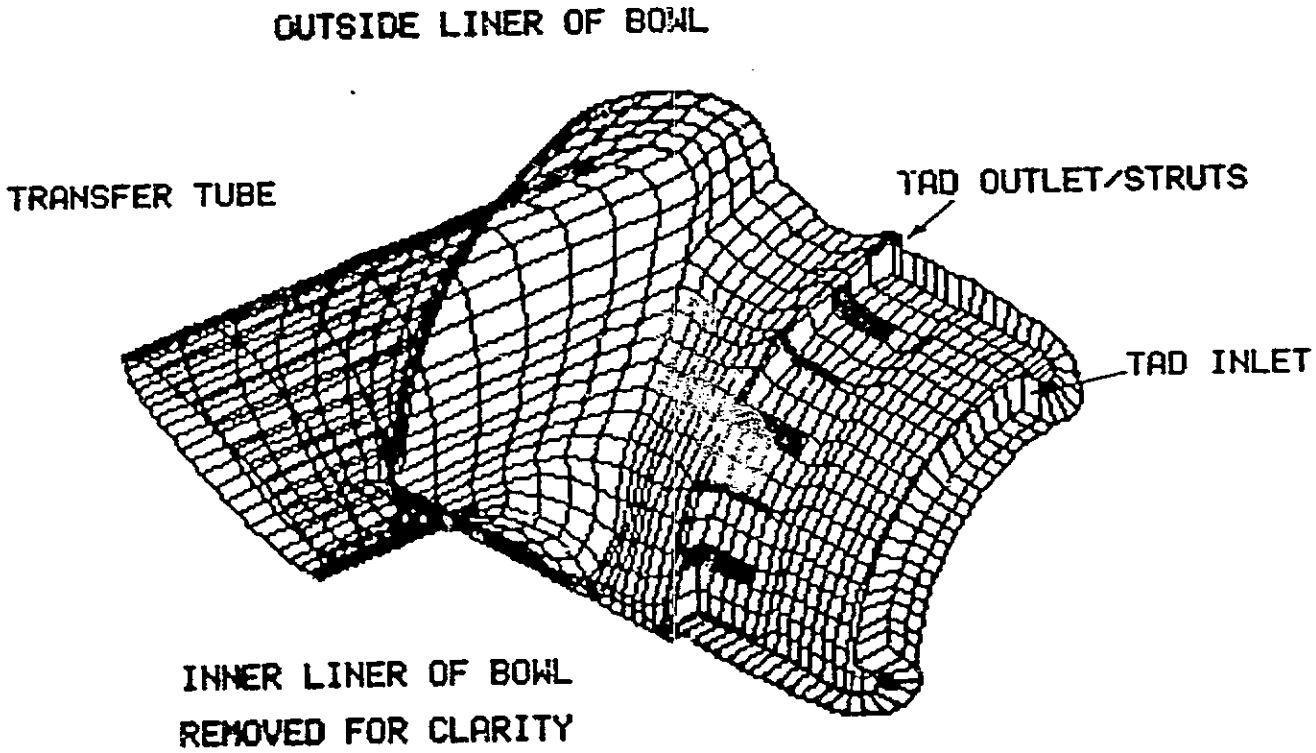

Fig. 4-2 View of Grid From Inside

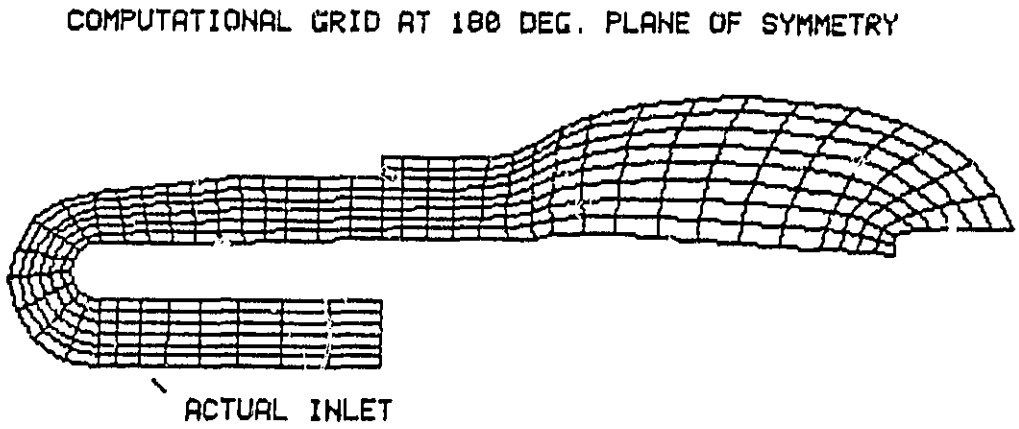

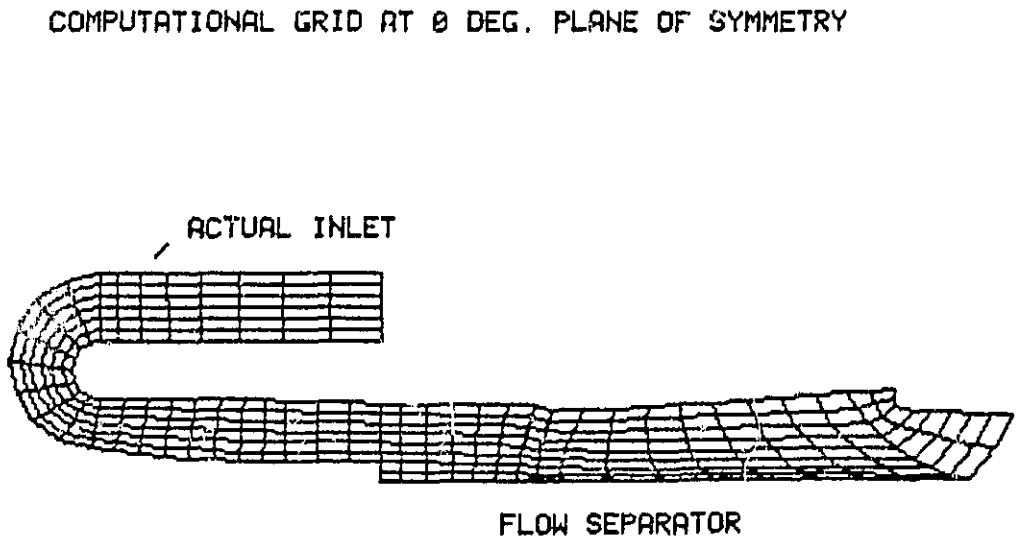

Fig. 4-3 Grids in Plane of Symmetry

4.5 Initial and Boundary Conditions

The inlet conditions prescribed in subsection 4.3 were applied to the artificially displaced inlet shown in Fig. 4-3. The viscosity of 10,000 times the molecular viscosity of air results in a Reynolds Number of 300 to 400 and, hence, laminar flow. Therefore a laminar parabolic velocity profile was superimposed on the average velocity distributed defined by Equation . .

No-slip boundary conditions were specified for all solid walls and tangency, or free-slip, boundary conditions were applied to the plane of symmetry. The mass flow rate in the exit plane of the transfer tube was held fixed at 72 lbm/sec. The total conditions at the inlet were held fixed, thereby allowing spurious signals to pass upstream and out of the problem.

4.6 Results

The flowfield for the TAD, HGM and transfer tube described above was computed using Continuum's VAST code. The problem required 11,000 time steps before a converged solution was obtained. The results of the study were presented in detail to the customer on November 28, 1984. A summary of the results will be discussed in this section.

The total pressure drop through the system is presented in Fig. 4-4 and shows a drop of 18 psi in the 180 bend of the turnaround duct, a 14 psi drop through the struts, and a total drop through the system of 48 psi. Static pressure drop through the system was about 35 psi. The pressure variation in the circumferencial direction in the HGM bowl inlet is shown in Fig. 4-5 and indicates a variation of 30 psi. Exactly how much of this result is affected by the assumed inlet pressure variation (8.38 psi) is unknown but it appears to be small.

The pressure distribution in the cross section in the plane of symmetry between the transfer tubes is presented in contour form in Fig. 4-6. The figure shows significant pressure drops in the 180° bend of the TAD and through the struts. The pressure variation in the bowl is small except in localized areas.

The pressure in the exit plane of the transfer tube varies only about 4 psi, hence, the exit plane pressure distribution is not presented in this discussion. Instead, velocity contours in the transfer tube are presented in Fig. 4-7 to show the nonuniform velocity distribution. A small area of high speed flow appears in the outer and upper portion of the tube.

Figures 4-4 through 4-7 show large pressure gradients in the turnaround duct and small pressure gradients in the transfer tube indicating an improved design over the 3 duct system currently in use.

5. CLOSURE

The analyses of single and multiple LOX posts will be continued. The laminar flow analysis of the TAD/HGM/transfer tubes was completed; the turbulent flow case will be analyzed in the next reporting period.

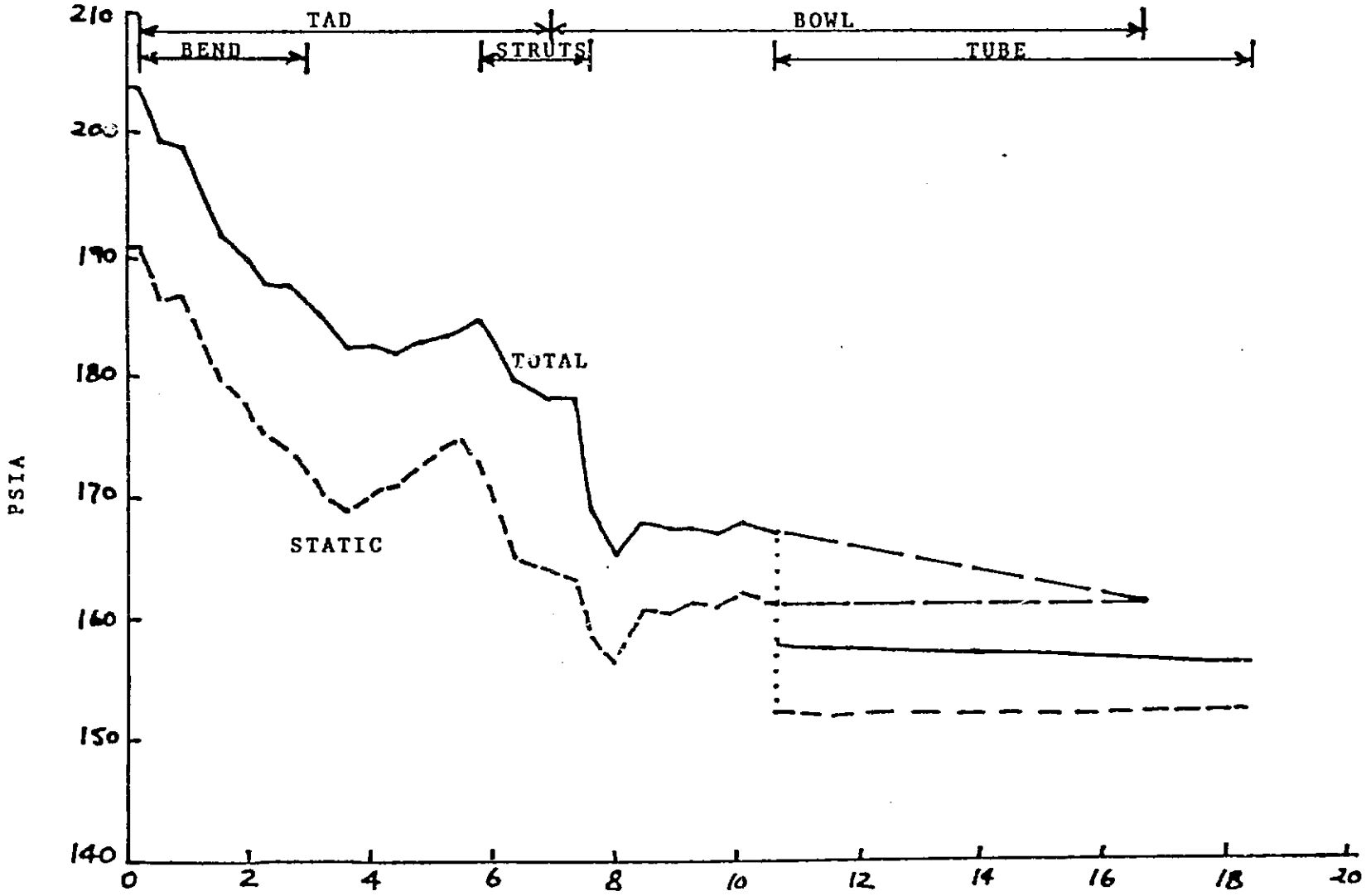

Fig. 4-4 Averaged Pressure in TAD/Bowl/Tube

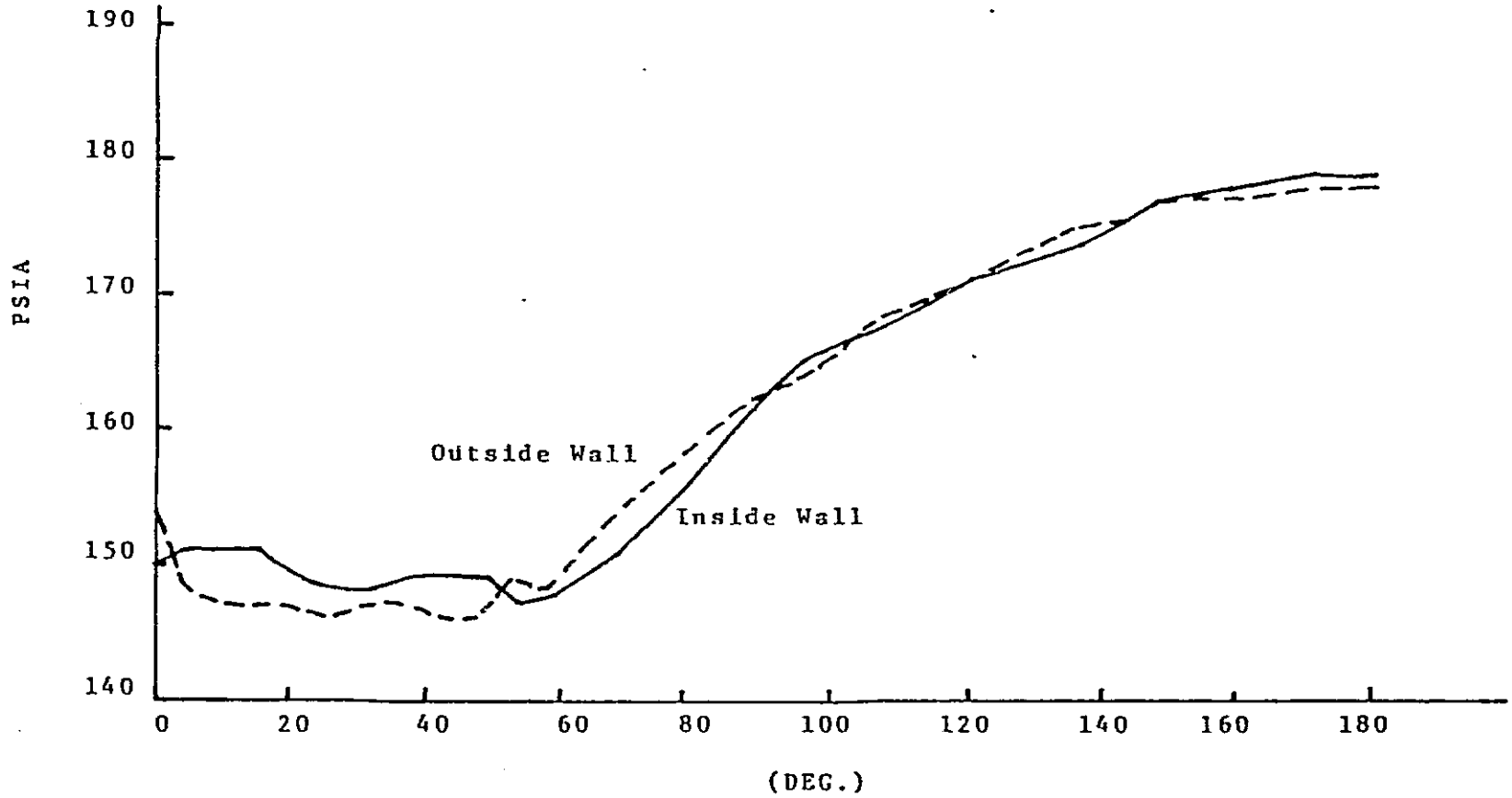

Fig. 4-5 Pressure Variation Around Bowl

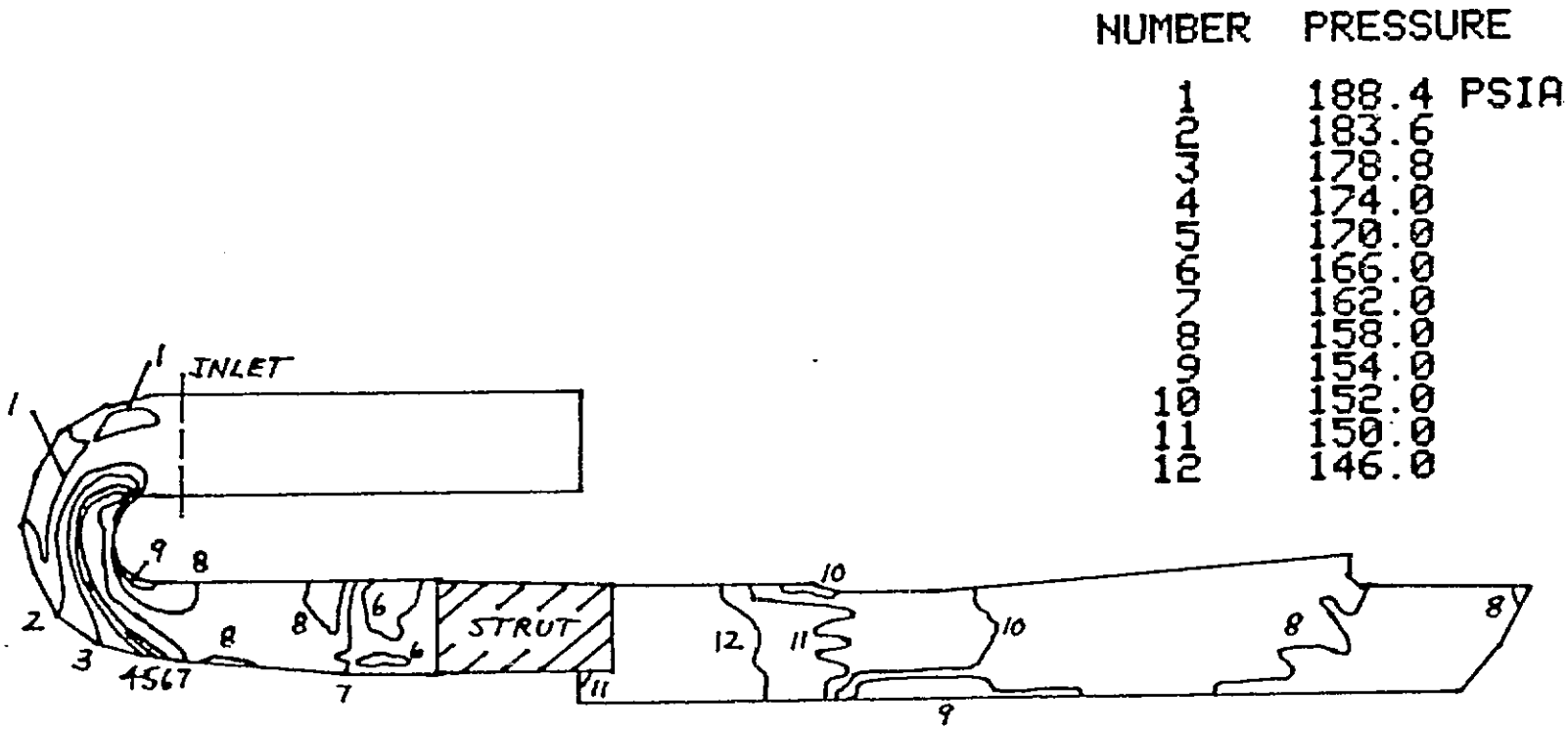

Fig. 4-6 Pressure Contours in TAD/Bowl at 0 Deg.

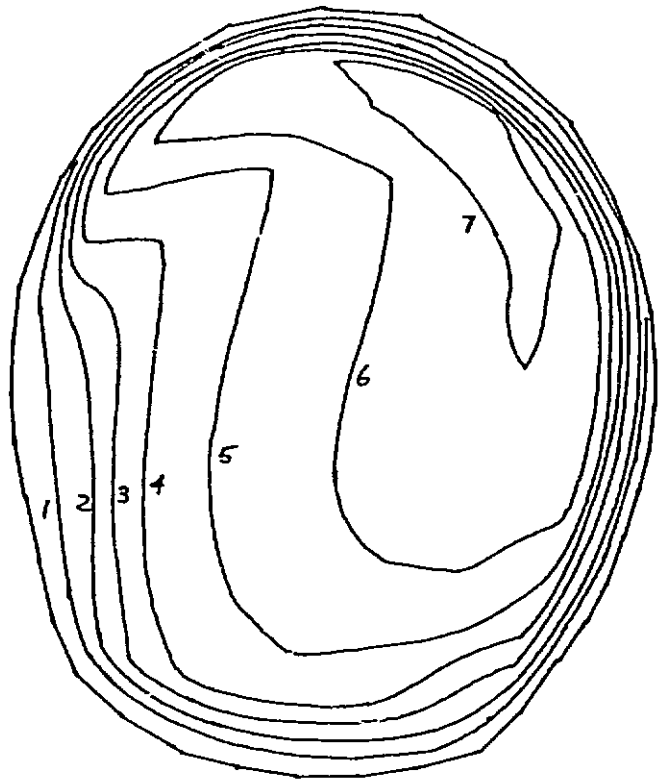

NUMBER	VELOCITY
1	44 FPS
7	308 FPS

Fig. 4-7 Velocity Contours Midway In Transfer Tube
(Looking into Tube from LOX Posts)